Atomic Spectroscopy

Article

Fast Determination of Gas Evolution Volume of Calcium Carbide by Laser-induced Breakdown Spectroscopy

Yuheng Shan,[‡a] Meng Wang,[‡b] An Li,[a] Xinyu Zhang,[a] Ying Zhang,[a] Xiaodong Liu,[a] and Ruibin Liu[a,*]

[a] Key Lab of Precision Spectroscopy and Optoelectronic Technology, School of Physics, Beijing Institute of Technology, Beijing 100081, P. R. China

[b] Xi'an University of Science and Technology, Xi'an 710054, P. R. China

Received: *July 26, 2023;* ***Revised:*** *October 17, 2023;* ***Accepted:*** *October 30, 2023;* ***Available online:*** *October 30, 2023.*

DOI: 10.46770/AS.2023.152

ABSTRACT: Calcium carbide is an important chemical raw material, and its gas evolution volume is a crucial indicator for its quality. However, the traditional methods to determine the gas evolution volume are costly and complicated. More important, it cannot be quantitatively detected with an in-situ real-time way. Herein, a totally new method to measure the gas evolution volume of calcium carbide based on Laser-induced breakdown spectroscopy (LIBS) is proposed for the first time. Tableting and pre-pulse were used to reduce the matrix effect. Moreover, the spectral pretreatments and standardization are necessary, including the removal of abnormal spectra, fitting and correction of background baselines and optimization of characteristic spectral line. Eventually, based on the principal component analysis combined with partial least squares method (PCA-PLS), a prediction model was successfully established, with the root mean square error of prediction set (RMSEP) of 1.498 L/kg. The average relative error of prediction set (AREP) is 0.48%. Our result illustrates that the LIBS provides a new solution for the rapid, accurate, and safe determination of gas evolution volume of calcium carbide.

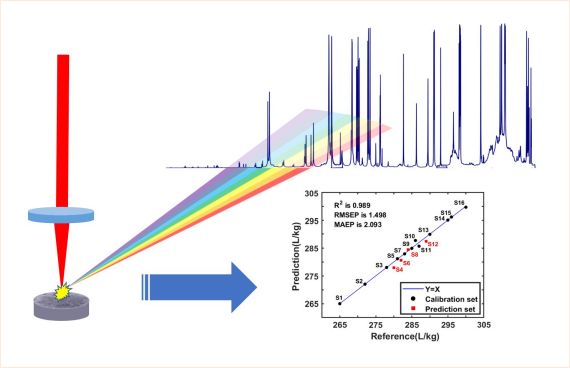

INTRODUCTION

Calcium carbide is a vital and fundamental chemical raw material, mainly used in acetylene gas production, lime nitrogen production, and as a desulfurizer in steel production. It has a wide range of significant applications in fields such as organic synthesis, industrial metallurgy, agricultural production. The gas evolution volume of calcium carbide, in L/kg, is defined as the volume of dry acetylene gas produced by the complete reaction of each kilogram of calcium carbide with sufficient water at a temperature of 20°C and a pressure of 101.3 kPa, which is a key indicator to evaluate the quality of calcium carbide. The primary method for measuring the gas evolution volume of calcium carbide is the "gas volumetric method", such as the method in the Chinese national standard "GB 10665-2004 Calcium Carbide".[1] This method quantifies the volume of acetylene produced by the reaction of calcium carbide with water via monitoring of gas pressure fluctuations within a specific equipment. Although the accuracy of this method is considerable (the absolute error for two parallel tests is less than 4 L/kg, mostly less than 2 L/kg), its equipment is unavoidably large and expensive. The process of this method is complex and time-consuming, as the gas meter requires periodical calibration and the entire experiment takes at least 30 minutes (including three parallel measurements). In addition, the robustness and reproducibility of the method are not ideal enough. Therefore, for its effective utilization, it is of great significance to develop a rapid, real-time, and high-precision method to measure gas evolution volume of calcium carbide.

Laser-induced breakdown spectroscopy (LIBS) is an analytical technique that utilizes a short-pulse laser to ablate the surface of samples, and subsequently collect emitted plasma radiation,

Table 1. Label and gas evolution volume of 16 calcium carbide samples

Label	S1	S2	S3	S4	S5	S6	S7	S8	S9	S10	S11	S12	S13	S14	S15	S16
Gas evolution volume (L/kg)	265	272	278	280	281	282	283	284	285	286	287	289	290	295	296	300

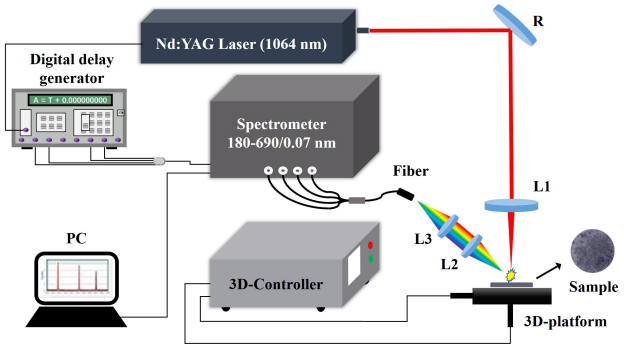

Fig. 1 Schematic diagram of the LIBS setup (R: reflector; L1, L2, L3: lens 1, 2, 3).

thereby the qualitative and quantitative determination of the composition and performance of samples can be realized. Due to its rapid detection capability, minimal sample damage, and relatively low cost, LIBS holds extensive and promising applications in various of fields including environmental monitoring,[2] coal detection,[3] food safety,[4] and energetic material analysis.[5] Therefore, the advantages of LIBS can effectively resolve the inherent limitations of current methods for measuring the gas evolution volume of calcium carbide.

Research on alternative methods for measuring gas evolution volume of calcium carbide beyond "gas volumetric method" is scarce. Zhou *et al.*[6] determined the gas evolution volume by measuring the changes in the mass of reactants within the instrument before and after the reaction, achieving an uncertainty of 2.61 L/kg, which is more accurate than traditional methods. There are few studies using LIBS to measure gas evolution volume of calcium carbide. In most studies using LIBS for quantitative analysis of materials such as metal ores and coal, the measurement of material composition and performance is achieved by combing LIBS with stoichiometric methods, including partial least squares (PLS) and support vector machine (SVM). Rifai *et al.*[7] used univariate calibration and PLS regression methods to quantitatively analyze six elements (copper, nickel, iron, cobalt, sulfur, and magnesium) in copper-nickel ore samples. The former method could only predict nickel and iron with moderate accuracy, while the latter was able to predict all elements and effectively improve the prediction accuracy of nickel and iron. In the study of Xu *et al.*,[8] by correcting PLS residuals through SVM, the root mean square error of prediction (RMSEP) of their semi-coke carbon content prediction model was reduced to 0.17%. By mixing binder into the semi-coke powder, the average RMSEP was kept at 1.89% in a three-day random test. Compared with basic PLS and direct painting, it effectively reduced the errors and improved the stability. Yuan *et al.*[9] combined PLS regression with principal component analysis (PCA) to measure the calorific value of air-dried coal. Compared with traditional PLS regression, the average relative error (ARE) of prediction model decreased from 3.55% to 2.71%, effectively improving the prediction accuracy.

This paper presents a novel approach for measuring the gas evolution volume of calcium carbide, which is more accurate and faster than the traditional method. The LIBS spectral data collected from calcium carbide samples were quantitatively analyzed by combining PCA with PLS regression. Firstly, by tableting the samples, the difficulty of spectra collection was reduced, and spectral stability was improved. Subsequently, a series of spectral pretreatments were carried out, including the removal of abnormal spectra, fitting and correction of background baselines, and optimization of characteristic spectral lines. These steps reduce spectral fluctuations caused by laser energy fluctuations and unstable ablation, while enhancing the representativeness of spectral data used for model training. Ultimately, modeling was completed based on 16 different samples, and the average relative error of prediction (AREP) was within 1%. Thus, this method provides a new effective method for the rapid and accurate measurement of the gas evolution volume of calcium carbide.

EXPERIMENTAL

Preparation of samples. As shown in Table 1, a total of 16 calcium carbide samples with gas evolution volumes ranging from 265 to 300 L/kg were selected and labeled as S1-S16. The gas evolution volumes of each sample was obtained through the Chinese national standard method.[1] Samples were pressed into tablets with a diameter of 13 mm and a thickness of 2 mm under a pressure of 15 MPa by using a mechanical powder tablet press (Tian Guang HY-12 type, Tianjin).

Experimental setup. LIBS measurements were conducted using the self-made setup in Fig. 1. A Q-switched Nd: YAG laser (Newwave, USA) at 1064 nm with a pulse duration of 3–5 ns and a repetition rate of 1–10 Hz was utilized as the ablation source. After getting reflected by the mirror (R), the laser pulse was focused onto the surface of sample by the lens (L1, f = 50 mm) with a spot diameter of approximately 80 μm at the focal, and generated a tremendous laser power density over 100 GW·cm^{-2}. After laser ablation, the emission spectra including the plasma

Fig. 2 A typical LIBS spectrum of calcium carbide.

Fig. 3 (a) Comparation of intensity absolute deviations of the characteristic peak (CaI504.16 nm) for pre-pulse and real-pulse. The subfigure of (a) is the distribution before sorting by deviation value. (b) Distribution of the intensities of the characteristic peaks (CaI504.16 nm), (c) electron density variations and (d) plasma temperature variations for samples in block and tablet.

continuous radiation and elemental atomic and ionic lines were acquired using a transverse signal collection module composed of two lenses (L2, f = 50 mm, L3, f = 75 mm) and a fiber (d = 200 μm). The spectra were then analyzed using a four-channel spectrometer installed with a CMOS detector (2048 × 2048 pixels, spectral resolution 0.07 nm, Avantes Avsdesktop USB3.0, Netherlands). The laser energy and integration time were optimized at 16 mJ and 30 μs, respectively. The gate of the spectrometer was controlled by a digital pulse delay generator (DG535, Stanford, USA) with the Q switch signal of laser pulse using as an external trigger source. The time delay from laser to the start of spectrum collection by the spectrometer was optimized to 1 μs. Under this parameter setting, the signal-to-noise ratio (SNR) was optimal.

To reduce the impact of laser energy fluctuations on spectral data, multiple spectra were averaged, collected from 10 repetitive pulses at 25 selected positions on each sample surface. To reduce the impact of sample surface differences, such as deliquescence, 10 ablation pulse were performed as pre-pulse at each of the 25 selected points before spectral collection. A total of 250 sets of spectral data were collected from 25 points on each sample surface.

RESULTS AND DISCUSSION

Figure 2 shows a typical spectrum of a representative calcium carbide sample (S1). Using the spectra database of the National Institute of Standards and Technology (NIST),[10] several spectral lines were determined, including the atomic and ionic spectral lines for calcium and the atomic spectral lines for carbon. Proper laser energy is important for spectral analysis. At lower irradiation laser energy, the spectral line intensity of carbon is relatively weak, and it is difficult to detect the spectral lines of impurity elements. Additionally, in order to obtain carbon atomic spectral lines during spectra collection, higher laser energy will cause some spectral lines of calcium to exceed the saturation intensity of the spectrometer, resulting in some unmarked high-intensity spectral lines in Fig. 2. The gas evolution volume of calcium carbide is determined by its CaC_2 content, which is significantly correlated with the spectral lines of carbon and calcium in the spectra of calcium carbide. As shown in Fig. 2, the rich spectral lines provide a foundation for quantitative analysis of LIBS spectral data based on machine learning methods.

Effect of tableting and pre-pulse on matrix effect. When calcium carbide is exposed to air, it will become unstable. The main component CaC_2 reacts with H_2O in the air and generates $Ca(OH)_2$, as shown in eq (1). Subsequently, $Ca(OH)_2$ on the surface of sample absorbs CO_2 from the air, and generates $CaCO_3$, as shown in eq (2).

$$CaC_2 + H_2O \rightarrow Ca(OH)_2 + C_2H_2 \quad (1)$$

$$Ca(OH)_2 + CO_2 \rightarrow CaCO_3 + H_2O \quad (2)$$

Chemical reactions and their products result in strong matrix effects in LIBS measurements. In addition, the uneven density distribution of calcium carbide blocks further enhances this matrix effect. The unevenness of composition and density between the surface and interior of materials is reflected in pronounced fluctuations in the collected spectra, which affects the accuracy and repeatability of quantitative analysis. In order to overcome the matrix effect of calcium carbide, especially in block samples, we performed tableting preparation and pre-pulse in our experiment.

In Fig. 3 (a), the characteristic peak (Ca I 504.16 nm) of S1 in tablet was selected as the analytical line, as it is the highest intensity Ca atomic spectral line without supersaturation in the spectrum of all samples. The absolute deviations of 250 pre-pulses and 250 real-pulses from the mean spectral intensity of all-pulses were calculated and sorted for each 250 measurements. The

Table 2. Parameters of the emission lines [a]

λ/nm	$A_{ki}/(10^8\ s^{-1})$	E_k/eV	g_k
Ca I 363.08	2.97	5.2996694	5
Ca I 364.44	3.55	5.3000005	7
Ca I 452.69	4.1	5.4470569	3
Ca I 504.16	3.3	5.1675384	3
Ca I 551.30	11	5.1808379	1

[a] From the spectra database of the NIST.

Fig. 4 Effect of each spectral pretreatment.

relative standard deviation (RSD) values of the characteristic peaks of the pre-pulse and the real-pulse are 30.76% and 15.49%, respectively, indicating that the fluctuation of spectral intensity of the pre-pulse is much greater than that of the real-pulse. As expected, due to the ability of pre-pulse to remove deliquescent products on the surface of calcium carbide samples, subsequent real-pulses can interact with actual calcium carbide. It can reduce the matrix effects caused by uneven composition, effectively improving the representativeness and stability of the spectra.

In laser induced plasma, the Stark broadening caused by electron radiation dominates the spectral line broadening.[11] The electron density is related to Stark broadening, so it can be estimated by eq (3):

$$\Delta\lambda_{1/2} = 2 \times 10^{-22} w n_e \qquad (3)$$

Where n_e is the electron density, $\Delta\lambda_{1/2}$ is the full width at half maximum of spectral line and w is the electron collision parameter. Herein, the electron density was calculated using CaI504.16 nm.

When the plasma satisfies the local thermodynamic equilibrium, the particles on the energy level obey the Boltzmann Distribution Law.[12] The spectral line intensity is related to the emissivity between energy levels. The plasma temperature can be estimated using Boltzmann plot, as shown in eq (4):

$$\ln\frac{I_\lambda}{g_k A_{ki}} = -\frac{1}{kT}E_k + c \qquad (4)$$

Where T is the plasma temperature, I_λ is the intensity of spectral line, g_k is the statistical weight of the upper energy level, A_{ki} is the transition probability, k is the Boltzmann constant and E_k is the energy of the upper energy level. The plasma temperature was fitted using the emission lines of Ca listed in Table 2.

In Fig. 3 (b), the RSD values of the characteristic peak (Ca I 504.16 nm) of the samples in original bulk and pressed tablets were 22.49% and 15.49%, respectively. As shown in Fig. 3 (c) and (d), there were also significant differences in the stability of electron density and plasma temperature of the samples before or after tableting pretreatment. The RSD values of electron density of block and tablet were 8.35% and 4.86%, respectively, while the RSD values of plasma temperature of block and tablet were 18.92% and 8.79%, respectively. The results indicate that the stability of laser-induced plasma and spectra in tablet sample is much higher than that in block sample, suggesting that the tableting preparation can reduce the matrix effect to some extent for the analysis of calcium carbide.

Spectral pretreatments. The deliquescence of calcium carbide samples will lead to deterioration and pulverization, causing the spectral fluctuations and reducing the reproducibility of data collection. Although preparations were made through tableting and pre-pulse ablation, some spectra still have errors beyond the range of systematic errors and random errors, which should be considered as data containing gross errors and removed as abnormal spectra. In order to reduce spectral fluctuations and improve prediction accuracy, we used the Pauta criterion[13] to remove abnormal spectra. The Pauta criterion assumes that the experimental data follows a normal distribution. By calculating the standard deviation of the data, data exceeding a certain confidence interval can be identified and processed. Herein, for a total of 250 sets of original spectral data from each of the 16 samples, the original spectral data is considered as X_{ij} (1×8192 matrix), where i is the number of samples and j is the number of sets. The spectra of sample center $\overline{X_{\imath jk}}$ (1×2048 matrix) is the median of total spectral intensity in each of the 4 sub-channel spectra, where k is the number of channels. For each spectrum of each sample, the Euclidean distance D_{ij} and corresponding residual error v_{ij} can be calculated using eqn (5) and (6). Then standard deviation σ_i^D of each sample can be calculated using equ (7), known as Bessel's formula. The data that satisfies equ (8) will be considered as an abnormal spectrum with gross errors, and will be deleted, as shown by the red curve in Fig. 4.

$$D_{ij} = \sum\nolimits_k \left(X_{ijk} - \overline{X_{\imath jk}}\right)^2 \qquad (5)$$

$$v_{ij} = D_{ij} - \frac{\sum_j D_{ij}}{250} \qquad (6)$$

Fig. 5 Effect of PCA. (a) The three-dimensional score plot for the first three principal components; (b) Interpretation rate and cumulative interpretation rate of each principal component.

$$\sigma_i^D = \sqrt{\frac{\sum_i {v_{ij}}^2}{250}} \quad (7)$$

$$v_{ij} > 3\sigma_i^D \quad (8)$$

$$\begin{cases} F(a_k) = b_k \\ F(a_k) = t_{k1} \cdot {a_k}^3 + t_{k2} \cdot {a_k}^2 + t_{k3} \cdot a_k + t_{k4} \\ F'_+(a_k) = F'_-(a_k) \\ F''_+(a_k) = F''_-(a_k) \end{cases}, \quad k \in [1,128] \quad (9)$$

$$F''(a_1) = F''(a_{128}) = 0 \quad (10)$$

$$S'_{ij} = S_{ij} - B'_{ij} \quad (11)$$

After removing abnormal spectra and recording or removing saturated spectral lines, 200 sets of spectral data were randomly selected for further analysis, as shown by the black curve in Fig. 4.

Due to the initial emission of laser-induced plasma accompanied by bremsstrahlung and compound radiation, there is always a strong continuous background in the spectrum. The proper delay time can be optimized to improve SNR as the continuous background radiation decays rapidly. However, the optimized spectrum still inevitably has a small amount of residual continuous background. In order to improve SNR and prediction accuracy, the spectrum is further removed by background baselines fitting and normalized. The combination of window translation smoothing[8] with cubic spline interpolation[14] effectively solves the issue of spectral information loss caused by Runge's phenomenon during high-order polynomial interpolation. Herein, for the 200 sets of selected spectral data from each of 16 samples, the data group S_{ijk} (1×64 matrix) is obtained by dividing the selected spectral data S_{ij} (1×8192 matrix) into 128 data groups with equal window width of 64, where k is the number of groups. The feature value b_{ijk} is the minimum value within its data group, and the feature value group B_{ij} (1×128 matrix) and position group A_{ij} (1×128 matrix) is obtained by arranging the feature values and their corresponding position. The background baseline B'_{ij} (1×8192 matrix) is obtained using eqn (9) and (10), known as cubic spline interpolation and the second type of boundary condition. The corrected spectral data S'_{ij} (1×8192 matrix) is obtained using eqn (11), as shown by the blue curve in Fig. 4.

Under the fundamental assumptions of uniform spatial distribution,[15] local thermodynamic equilibrium,[16] stoichiometric ablation,[17] and optical thinness[18] in laser-induced plasma, the characteristic spectral lines can be considered to have a close correlation with the element content, thereby their intensity can be used for quantitative analysis. In order to enhance the signal contrast and representativeness of spectral lines and improve prediction accuracy, the spectral standardization was further carried out, including spectral line discrimination, non-peak zeroing, peak shift correction, and abnormal peak correction. Herein, for the 200 sets of corrected spectral data from each of 16 samples, the characteristic peak value p_{ijk} is every peak of S'_{ij} greater than three times the standard deviation of the background baseline, where k is the number of peaks. The matrix of characteristic peaks P_{ij} (1×8192) is obtained by zeroing all pixel in S'_{ij} except p_{ijk}. For each peak pixel of P_{ij} in all sets of spectra from the same sample, the number of peaks on it and its two adjacent pixels on the left and right are compared. The peak position is located on the peak pixel with the highest number of peaks. The peak value of adjacent pixels is then shifted to the correct peak position. On the one hand, peak positions with peak occurrence frequencies below 10% are determined as accidental peaks. Subsequently, such peak positions are eliminated and the corresponding peak values are reset to zero. On the other hand, the absence of peak values at peak positions with peak occurrence frequencies above 90% are determined as a loss of peak intensity.

Fig. 6 (a) Gas evolution volume prediction models based on PCA-PLS. (b) The effect of tableting, pre-pulse, and spectral pretreatments on quantitative analysis errors.

Table 3. Model evaluation indices of gas evolution volume prediction model

Model evaluation indices	Calibration set	Prediction set
ARE	0.12%	0.48%
RMSE	0.640 L/kg	1.498 L/kg
MAE	1.70 L/kg	2.09 L/kg

Afterwards, the missing peak fitting intensity is calculated using PLS regression method based on other high correlation peaks (R2 > 0.9) in the same set of spectral data, and added to the loss of peak intensity. Thus, the final spectra to be analyzed are obtained by averaging the optimized characteristic matrix P'_{ij}, as shown by green stem in Fig. 4.

Gas evolution volume prediction model for calcium carbide. Finally, the prediction model for the gas evolution volume of calcium carbide was established based on partial least squares regression combined with principal component analysis (PCA-PLS).[19] PCA was used to reduce the dimensionality of all pretreated spectral data. Fig. 5(a) shows the three-dimensional scores for the first three principal components. None of the spectral data of all 16 samples exceed the 95% confidence interval for Hotelling T^2 statistical test,[20] indicating that there were no significant outliers in all samples, and PLS regression modeling could be performed on the entire samples set.

Firstly, 12 samples were randomly selected as the calibration set, while the remaining 4 samples were used as the prediction set, without participating in model training. In PLS regression, when the number of principal components is insufficient, the interpretation rate of the original data is inadequate to fully reflect the characteristics of the original data, resulting in lower prediction accuracy. When the number of principal components is excessive, overfitting occurs and prediction accuracy decreases. In Fig. 5 (b), the interpretation rates of the top 10 principal components are 37.02%, 30.95%, 14.86%, 6.69%, 3.47%, 2.52%, 1.39%, 1.10%, 0.58%, and 0.48%, respectively. The cumulative interpretation rate of the first seven principal components reached 95.80%, exceeding 95%, indicating that the first seven principal components cover most of the information in the spectral data of calcium carbide. Therefore, seven principal components were selected for model training.

The prediction model of gas evolution volume of calcium carbide is shown in Fig. 6 (a). The standard values come from experimental data obtained using the traditional method, while the prediction values are derived from our model. Model evaluation indicators, including model goodness of fit (R^2), average relative error of calibration set (AREC), root mean square error of calibration set (RMSEC), maximum absolute error of calibration set (MAEC), average relative error of prediction set (AREP), RMSEP, and maximum absolute error of prediction set (MAEP), are illustrated in Table 3. The established gas evolution prediction model has R^2 of 0.988, with an AREP less than 5% and a RMSEP less than 1.5 L/kg. Notably, the MAEP is 2.09 L/kg, which is far less than the absolute error requirement of two parallel tests in the national standard method (4 L/kg).[1] At the same time, we compared the effect of tableting, pre-pulse, and all spectral pretreatments on the prediction model, as shown in Fig. 6 (b). The results indicate that all these methods can effectively reduce analysis errors, including RMSEP and MAE, and improve prediction accuracy. The good prediction results validate the effectiveness of this method for measuring gas evolution volume of calcium carbide based on LIBS.

CONCLUSION

In this paper, we propose a new method based on LIBS to measure the gas evolution volume of calcium carbide. Tableting and pre-pulse, as well spectral pretreatments were applied to improve

prediction accuracy. Outliers in spectra were removed to reduce spectral fluctuation, and the spectra were corrected by fitting the background baseline to improve SNR. Additionally, characteristic spectral lines were optimized to enhance the signal contrast and representativeness. An effective PCA-PLS prediction model was established with R2, RMSEP and AREP of 0.989, 1.498 L/kg and 0.48%, respectively, which verify the high-accuracy and fast way to determine the gas evolution volume of calcium carbide is feasible. Therefore, LIBS has a potential to be applied on accurate gas evolution detection, and meet the industrial requirements of online analysis of calcium carbide.

ASSOCIATED CONTENT

The supporting information (Figs. S1−S5) is available at www.at-spectrose.com/as/home.

AUTHOR INFORMATION

Ruibin Liu received his PhD in 2007 from Institute of Physics, Chinese Academy of Sciences. He is a professor at the School of Physics at Beijing Institute of Technology. His work covers a range of topics, from the interaction and microscopic reaction kinetics between light and energetic materials, to laser material identification techniques. He has published over 130 papers, mainly devoted to the development of precision laser spectroscopy and technology for industrial and national defense applications.

Corresponding Author

* R. B. Liu

Email address: liusir@bit.edu.cn

‡ Yuheng Shan and Meng Wang contributed equally to this work.

Notes

The authors declare no competing financial interest.

ACKNOWLEDGMENTS

The authors gratefully thank the National Key Research and Development Project (2018YFC2001100) for financial support of this work.

REFERENCES

1. Standardization Administration of the People's Republic of China, GB/T 10665-2004 Calcium Carbide, 2014.
2. R. Wainner, R. Harmon, A. Miziolek, K. McNesby, and P. French, *Spectrochim. Acta B*, 2001, **56**, 777–793. https://doi.org/10.1016/S0584-8547(01)00229-4
3. G. Pan, J. Lu, M. Dong, S. Yao, and Z. Xie, *Plasma Sci. Technol.*, 2015, **17**, 625–631. https://iopscience.iop.org/article/10.1088/1009-0630/17/8/03
4. M. Yao, H. Yang, L. Huang, T. Chen, G. Rao, and M. Liu, *Appl. Optics*, 2017, **56**, 4070–4075. https://doi.org/10.1364/AO.56.004070
5. X. Wang, R. Liu, Y. He, Y. Fu, J. Wang, A. Li, X. Guo, M. Wang, W. Guo, and T. Zhang, *Opt. Express*, 2022, **30**, 4718–4736. https://doi.org/10.1364/oe.449382
6. Z. Zhou and F. Li, *Metrology Science and Technolog*, 2012. **3**, 10–11,16. https://d.wanfangdata.com.cn/periodical/ChlQZXJpb2RpY2FsQ0hJTmV3UzIwMjMwODMxEg1qbGpzMjAxMjA5MDAzGghmZzdtd3J3aw%253D%253D
7. Kheireddine Rifai, Lütfü Özcan, François Doucet, François Vidal, *Spectrochim. Acta B*, 2020, **165**, 105766–105772. https://doi.org/10.1016/j.sab.2020.105766
8. X. Xu, A. Li, X. Wang, C. Ding, S. Qiu, Y. He, T. Lu, F. He, B. Zou, and R. Liu, *J. Anal. At. Spectrom.*, 2020, **35**, 984–992. https://doi.org/10.1039/c9ja00443b
9. T. Yuan, Z. Wang, S.-L. Lui, Y. Fu, Z. Li, J. Liu, and W. Ni, *J. Anal. At. Spectrom.*, 2013, **28**, 1045–1053. https://doi.org/10.1039/c3ja50097g
10. A. Kramida, Y. Ralchenko, J. Reader, and N. A. Team. National Institute of Standards and Technology: Gaithersburg, 2021. https://dx.doi.org/10.18434/T4W30F
11. H. R. Griem and W. L. Barr, *IEEE T. Plasma Sci.*, 1975, **3**, 227–227, https://doi.org/10.1109/TPS.1975.4316912
12. B. Bousquet, V. Gardette, V. M. Ros, R. Gaudiuso, M. Dell'Aglio, and A. De Giacomo, *Spectrochim. Acta B*, 2023, **204**, 106686–106695. https://doi.org/10.1016/j.sab.2023.106686
13. Z. Wang, L. Li, L. West, Z. Li, and W. Ni, *Spectrochim. Acta B*, 2012, **68**, 58–64. https://doi.org/10.1016/j.sab.2012.01.005
14. S. He, S. Fang, X. Liu, W. Zhang, W. Xie, H. Zhang, D. Wei, W. Fu, and D. Pei, *Chemometr. Intell. Lab.*, 2016, **152**, 1–9. https://doi.org/10.1016/j.chemolab.2016.01.005
15. C. A. D'Angelo, D. M. D. Pace, G. Bertuccelli, and D. Bertuccelli, *Spectrochim. Acta B*, 2008, **63**, 367–374. https://doi.org/10.1016/j.sab.2007.10.049
16. O. Barthélemy, J. Margot, S. Laville, F. Vidal, M. Chaker, B. Le Drogoff, T. W. Johnston, and M. Sabsabi, *Appl. Spectrosc.*, 2005, **59**, 529–536. https://doi.org/10.1366/0003702053641531
17. C. C. Garcia, H. Lindner, A. von Bohlen, C. Vadla, and K. Niemax, *J. Anal. At. Spectrom.*, 2008, **23**, 470–478. https://doi.org/10.1039/b718845e
18. T. Li, Z. Hou, Y. Fu, J. Yu, W. Gu, and Z. Wang, *Anal. Chim. Acta*, 2019, **1058**, 39–47. https://doi.org/10.1016/j.aca.2019.01.016
19. A. Li, X. Zhang, Y. Yin, X. Wang, Y. He, Y. Shan, Y. Zhang, X. Liu, L. Zhong, and R. Liu, *J. Anal. At. Spectrom.*, 2023, **38**, 810–817. https://doi.org/10.1039/d3ja00020f
20. K. V. Mardia, *J. R. Stat. Soc. C-Appl.*, 1975, **24**, 163–171. https://doi.org/10.2307/2346563